

1 **Triplex and other DNA motifs show motif-specific associations with** 2 **mitochondrial DNA deletions and species lifespan.**

3 **Authors**

4 Kamil Pabis¹

5 1. Georg August University of Göttingen, Göttingen, Germany.

6 Mail: Kamil.pabis@gmail.com

7

8

9 **ABSTRACT**

10 The “theory of resistant biomolecules” posits that long-lived species show resistance to molecular
11 damage at the level of their biomolecules. Here, we test this hypothesis in the context of mitochondrial
12 DNA (mtDNA) as it implies that predicted mutagenic DNA motifs should be inversely correlated with
13 species maximum lifespan (MLS).

14 First, we confirmed that guanine-quadruplex and direct repeat (DR) motifs are mutagenic, as they
15 associate with mtDNA deletions in the human major arc of mtDNA, while also adding mirror repeat (MR)
16 and intramolecular triplex motifs to a growing list of potentially mutagenic features. What is more,
17 triplex motifs showed disease-specific associations with deletions and an apparent interaction with
18 guanine-quadruplex motifs.

19 Surprisingly, even though DR, MR and guanine-quadruplex motifs were associated with mtDNA
20 deletions, their correlation with MLS was explained by the biased base composition of mtDNA. Only
21 triplex motifs negatively correlated with MLS even after adjusting for body mass, phylogeny, mtDNA
22 base composition and effective number of codons.

23 Taken together, our work highlights the importance of base composition for the comparative
24 biogerontology of mtDNA and suggests that future research on mitochondrial triplex motifs is
25 warranted.

26 **ABBREVIATIONS**

27 BPs, mtDNA deletion break points

28 DR, direct repeats

29 ER, everted repeats

30 GQ, guanine-quadruplexes

31 IR, inverted repeats

32 MLS, species maximum lifespan

33 MR, mirror repeats

34 nBMST, non-B DNA motif search tool

35 Nc, number of effective codons

- 36 PGLS, phylogenetic generalized least squares
- 37 SD, standard deviation
- 38 Trip, Triplex forming motif
- 39 XR, any repeat half-site or motif
- 40 mtDNA, mitochondrial DNA

41 INTRODUCTION

42 Macromolecular damage to lipids, proteins and DNA accumulates with aging (**Richardson and Schadt**
43 **2014, Gladyshev 2013**), whereas cells isolated from long-lived species are resistant to genotoxic and
44 cytotoxic drugs, giving rise to the multistress resistance theory of aging (**Miller 2009, Hamilton and**
45 **Miller 2016**). By extension of this idea, the “theory of resistant biomolecules” posits that lipids, proteins
46 and DNA itself should be resilient in long-lived species (**Pamplona and Barja 2007**). In support of this
47 theory, it was shown that long-lived species possess membranes that contain fewer lipids with reactive
48 double bonds (**Valencak and Ruf 2007**) and perhaps a lower content of oxidation-prone cysteine and
49 methionine in mitochondrially encoded proteins (see **Aledo et al. 2012** for a discussion).

50 Mitochondrial DNA (mtDNA) mutations constitute one type of macromolecular damage that
51 accumulates over time. Point mutations accumulate in proliferative tissues like the colon and in some
52 progeroid mice (**Kaupila et al. 2017**), while the accumulation of mtDNA deletions in postmitotic tissues
53 may underpin certain age-related diseases like Parkinson’s and sarcopenia (**Lawless et al. 2020, Bender**
54 **et al. 2006**).

55 If the theory of resistant biomolecules can be generalized, the mtDNA of long-lived species should resist
56 both point mutation and deletion formation. However, we will focus on deletions because they are
57 more pathogenic than point mutations at the same level of heteroplasmy (**Gamange et al. 2014**) and
58 human tissues do not accumulate high levels of point mutations observed in progeroid mouse models
59 (**Khrapko et al. 2006**).

60 Since deletion formation depends on the primary sequence of the mtDNA (sequence motifs) it is
61 amenable to bioinformatic methods. Ever since a link between direct repeat (DR) motifs and deletion
62 formation became known, variations of the theory of resistant biomolecules have been tested, although
63 not necessarily under this name. It was reasoned that long-lived species evolved to resist deletion
64 formation and mtDNA instability by reducing the number of mutagenic motifs in their mtDNA
65 (**Khaidakov et al. 2006, Yang et al. 2013**).

66 We aim to extend these findings by re-evaluating and establishing new candidate motifs, which we then
67 correlate with species maximum lifespan (MLS). Studying multiple motif classes at once also allows us to
68 reveal relationships between potentially overlapping mtDNA motifs that may affect the data. We define
69 candidate motifs as those that are associated with deletion formation inside the major arc of human
70 mtDNA, because during asynchronous replication the major arc is single stranded for extended periods
71 of time (**Persson et al. 2019**) which should favor the formation of secondary structures. Finally, we test if
72 these motifs correlate with the MLS of mammals, birds and ray-finned fishes after correcting for
73 potential biases, especially global mtDNA base composition which is an important confounder (**Aledo et**
74 **al. 2012**) yet is neglected in some studies (**Yang et al. 2013**).

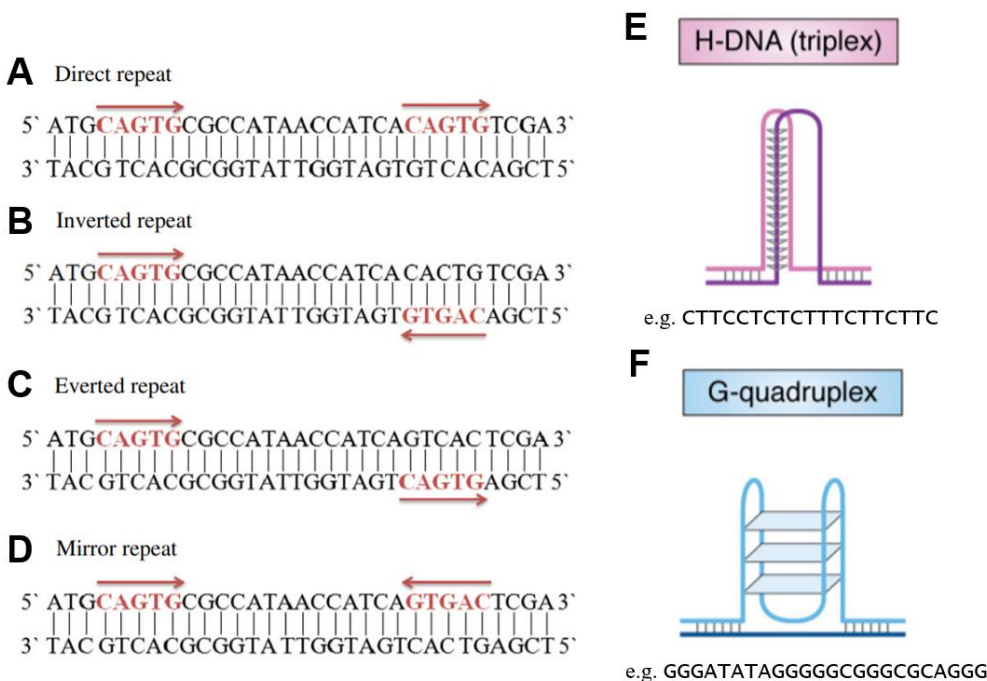
75 The choice of motifs to study is based on biological plausibility and published literature that will be
76 briefly reviewed below. Mutagenic motifs include repeats as well as guanine-quadruplex (GQ)- and
77 triplex-forming motifs. DR motifs can lead to DNA instability through strand-slippage if two DR motifs
78 mispair during replication (**Persson et al. 2019**). Whereas inverted repeat (IR), G-quadruplex and triplex
79 motifs destabilize progression of the replication fork through the formation of stable secondary
80 structures. Some of the structures formed include hairpins for IR motifs (**Tremblay-Belzile et al. 2015**),
81 triple stranded DNA for triplex motifs and bulky stacks of guanines for G-quadruplex motifs (**Bacolla et**

82 **al. 2016; Fig. 1**. Mirror repeat (MR) and everted repeat (ER) motifs, in contrast, do not allow stable
 83 Watson-Crick base pairing and are thus less likely to be mutagenic, although a subset of MR motifs may
 84 form triplex structures (**Kamat et al. 2016**).

85 Thus, many motifs can be mutagenic in principle, but what is the evidence that these motifs are related
 86 to mtDNA instability, particularly deletions, and MLS?

87 Paradoxically, while DRs are the motif most consistently associated with mtDNA deletion breakpoints
 88 (BPs), despite preliminary reports (**Khaidakov et al. 2006, Lakshmanan et al. 2012, Yang et al. 2013**), no
 89 correlation with species MLS was seen in recent studies (**Lakshmanan et al. 2015**). In contrast, with the
 90 exception of one preprint (**Mikhailova et al. 2020**), IRs are not known to be associated with mtDNA
 91 deletions (**Dong et al. 2014**), although they do show a negative relationship with species MLS (**Yang et**
 92 **al. 2013**) and may contribute to inversions (**Tremblay-Belzile et al. 2015**). Whether age-related mtDNA
 93 inversions underlie any pathology, however, requires further study. Finally, G-quadruplex motifs are
 94 associated with both deletions (**Dong et al. 2014**) and point mutations (**Butler et al. 2020**), but no study
 95 tested if they correlate with MLS. Triplex motifs are poorly studied with one report finding no
 96 association between these motifs and deletions (**Oliveira et al. 2013**).

97 Based on these studies we decided to test the theory of resistant biomolecules by quantifying DR, MR,
 98 IR, ER, G-quadruplex- and triplex-forming motifs. We stipulate that if a motif class played a causal role in
 99 aging, it should be involved in deletion formation and its abundance should be negatively correlated
 100 with species MLS.



101
 102 **Figure 1**
 103 A. Direct repeat, both half-sites have the same orientation.
 104 B. Inverted repeat, the half-sites are complementary and has mirror symmetry.

105 C. Everted repeat, the half-sites are complementary.

106 D. Mirror repeat, the half-sites have mirror symmetry.

107

108 E. Triplex motifs can form a triple helical DNA structure also called H-DNA.

109 F. In a G-quadruplex multiple G-quartets (depicted as blue rectangles) stack on top of each other.

110 Adapted from **Gurusaran et al. (2013)** and **Khristich and Mirkin (2020)** with permission. Half-sites
111 shown in red.

112 **METHODS**

113 **Detection of DNA motifs**

114 Repeats were detected by a script written in R (vR-3.6.3). Briefly, to find all repeats with N basepairs
115 (bps), the mtDNA light strand is truncated by 0 to N bps and each of the N truncated mtDNAs is then
116 split every N bps. This generates every possible substring (and thus repeat) of length N. In the next step,
117 duplicate strings are removed. Afterwards we can find DR (a substring with at least two matches in the
118 mtDNA), MR (at least one match in the mtDNA and on its reverse), IR (at least one match in the mtDNA
119 and on its reverse-complement) and ER motifs (at least one match in the mtDNA and on its
120 complement). Overlapping and duplicate repeats were not counted for the correlation between repeats
121 and MLS. The code for the analyses performed in this paper can be found on github
122 (pabisk/aging_triplex2).

123 Unless stated otherwise, all analyses were performed in R. G-quadruplex motifs were detected by the
124 pqsfinder package (v2.2.0, **Hon et al. 2017**). Intramolecular triplex-forming motifs were detected by the
125 triplex package (v1.26.0, **Hon et al. 2013**) and duplicates were removed. We also compared the data
126 with two other publicly available tools, Triplexator (**Buske et al. 2013**), and with the non-B DNA motif
127 search tool (nBMST; **Cer et al. 2011**). Triplexator was run on a virtual machine in an Oracle VM
128 VirtualBox (v6.1) in -ss mode on the human mitochondrial genome and its reverse complement, the
129 results were combined and overlapping motifs from the output were removed. We used the web
130 interface of nBMST to detect mirror repeats/triplexes (v1.0).

131 **Association between motifs and major arc deletions**

132 The major arc was defined as the region between position 5747 and 16500 of the human mtDNA
133 (NC_012920.1). The following deletions and their breakpoints were located in this region and included:
134 1066 deletions from the MitoBreak database (**Damas et al. 2014, mtDNA Breakpoints.xlsx**), 1114 from
135 **Persson et al. (2019)** and 1894 from **Hjelm et al. (2019)**.

136 Each deletion is defined by two breakpoints. A breakpoint pair was considered to associate with a motif
137 if the motif fell within a defined window around one or both breakpoints, depending on the analysis.
138 The window size was chosen in relation to the length of the studied motifs (30 bp for repeats and 50 bp
139 for other motifs).

140 Three different motif orientations relative to the breakpoints were considered. Two orientations for
141 motifs with half-sites (i.e. repeats), either both half-sites at any one breakpoint of a deletion, or one
142 half-site per breakpoint of a deletion. Motifs with overlapping half-sites were not counted. In the third
143 case, distinct G-quadruplex and triplex motifs could associate with one or both breakpoints of a deletion,
144 but were at most counted once, since the latter case is sufficiently rare.

145 In order to exclude overlapping “hybrid” motifs, MR and DR motifs with the same sequence were
146 removed whereas triplex and G-quadruplex motifs were removed if they were in proximity.

147 To generate controls, the mtDNA deletions as a whole were randomly redistributed inside the major arc
148 which, because of the fixed deletion size, allowed us to approximate the original distribution of
149 breakpoints (as suggested by **Oliveira et al. 2013**). Significance was determined via one-sample t-test in
150 Prism (v7.04) by comparing actual breakpoints to 20 such randomized controls. Alternative controls
151 were generated by shifting each breakpoint by 200 bp towards the midpoint of the major arc or as in
152 **Fig. S9**.

153 **Cancer associated breakpoints**

154 We obtained all autosomal breakpoints available from the Catalogue Of Somatic Mutations In Cancer
155 (COSMIC; release v92, 27th August 2020), which includes deletions, inversions, duplications and other
156 abnormalities (n=587515 in total). After removing breakpoints whose sequences could not be retrieved
157 (<1.7%), we quantified the number of predicted G-quadruplex and triplex motifs in a 500 bp window
158 centered on the breakpoints using default settings for the detection of these motifs. Sequences of
159 breakpoint regions were obtained from the GRCh38 build of the human genome using the BSgenome
160 package (v1.3.1). Each breakpoint shifted by +3000 bps served as its own control.

161 **Lifespan, base composition and life history traits**

162 We included three phylogenetic classes in our analysis for which we had sufficient data (n>100),
163 mammals, birds and ray-finned fishes (actinopterygii). MLS and body mass were determined from the
164 AnAge database (**Tacutu et al. 2018**) and, for mammals, supplemented with data from **Pacifici et al.**
165 **(2013)**. The mtDNA accessions were obtained from an updated version of MitoAge (unpublished; **Toren**
166 **et al. 2016**). Species were excluded if body mass data was unavailable, if the sequence could not be
167 obtained using the genbankr package (v1.14.0), or if the extracted cytochrome B DNA sequence did not
168 allow for an alignment, precluding phylogenetic correction. The species data can be found in the
169 supplementary (**Species Data.xlsx**).

170 We analyzed the full mtDNA sequence, heuristically defined as the mtDNA sequence between the first
171 and last encoded tRNA, excluding the D-loop, which is rarely involved in repeat-mediated deletion
172 formation (**Yang et al. 2013**). The effective number of codons was calculated using Wright’s Nc (**Smith et**
173 **al. 2019**). Base composition was calculated for the light-strand. GC skew was calculated as the fraction
174 $(G - C)/(G + C)$ and AT skew as $(A - T)/(A + T)$. All correlations are Pearson’s R. Partial correlations were
175 performed using the ppcor package (v1.1).

176 **Phylogenetic generalised least squares and phylogenetic correction**

177 Observed correlations between traits and lifespan can be spurious due to shared species ancestry
178 (**Speakman 2005**). To correct for this, we use phylogenetic generalised least squares (PGLS)
179 implemented in the caper package (v1.0.1). Species phylogenetic trees were constructed via neighbor
180 joining based on aligned cytochrome B DNA sequences using Clustal Omega from the msa package
181 (v1.18.0) and in the resulting mammalian and bird tree, four branch edge lengths were equal to zero,
182 which were set to the lowest non-zero value in the dataset.

183

184 **RESULTS**

185 **Direct repeats and mirror repeats are over-represented at mtDNA deletion breakpoints**

186 In order to define candidate mtDNA motifs that could be linked with lifespan, we started by reanalyzing
187 motifs that associate with mtDNA deletion breakpoints reported in the MitoBreak database (**Damas et**
188 **al. 2014; Fig. S1; mtDNA Breakpoints.xlsx**). In the below analysis, we consider DR and IR motifs thought
189 to be mutagenic, as well as MR and ER motifs, so far not known to be mutagenic and we pool all 6 to 15
190 bp long repeats, since the data is similar between different repeat lengths (**Fig. S2**).

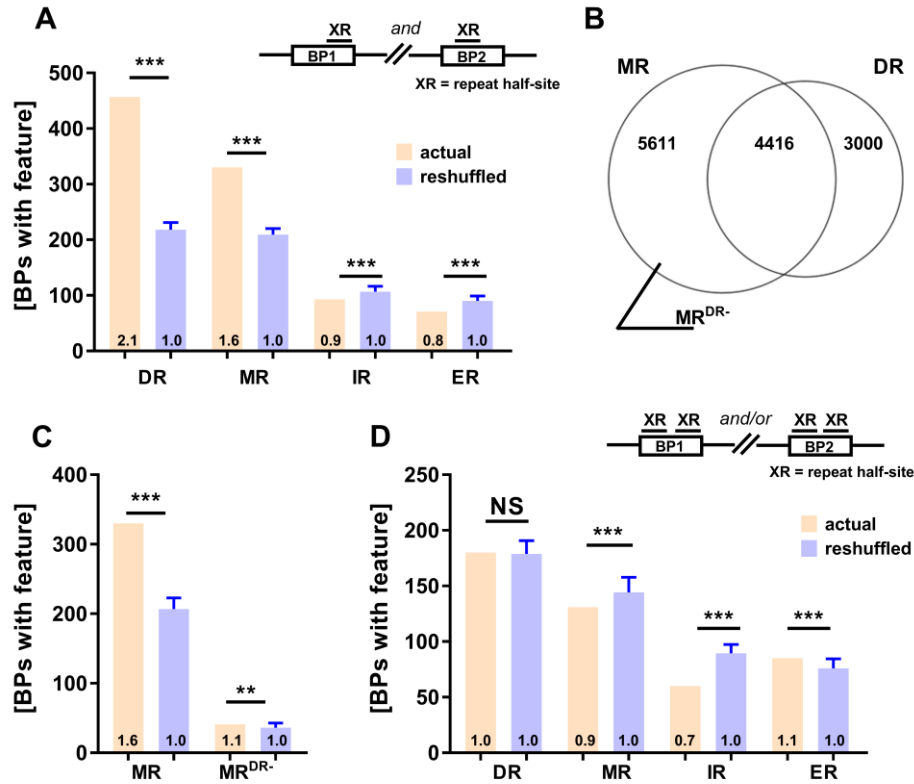
191 As shown by others, we found that DR motifs often flank mtDNA deletions (**Fig. 2A**). In contrast, no
192 strong association was seen for ER and IR motifs, even considering a larger window around the
193 breakpoint to allow for the fact that IRs could bridge and destabilize mtDNA over long distances
194 (**Persson et al. 2019; Fig. S3**).

195 Surprisingly, we also found MR motifs flanking deletion breakpoints more often than expected by
196 chance (**Fig. 2A**). However, DR and MR motifs are known to correlate with each other (**Shamanskiy et al.**
197 **2019; Fig. 5B**) and indeed we noticed a large sequence overlap between MR and DR motifs (**Fig. 2B**),
198 which could explain an apparent over-representation of MRs at breakpoints. Removal of overlapping
199 MR-DR hybrid motifs confirmed this suspicion. After this correction, the degree of enrichment was
200 strongly attenuated (**Fig. 2C**) and the total number of breakpoints flanked by MR motifs was reduced
201 by >80%. Nevertheless, long MR motifs remained particularly over-represented around deletions (**Fig.**
202 **S4**).

203 Since the prior analysis only considered motifs that flank both breakpoints, we next tested the idea that
204 IR and other motifs could be mutagenic if both half-sites are found at any of the breakpoints. However,
205 in this analysis no motif class showed enrichment around breakpoints (**Fig. 2D**).

206

207



208

209 Figure 2

210 Direct repeat (DR) and mirror repeat (MR) motifs are significantly enriched around actual deletion
 211 breakpoints (BPs) compared to reshuffled BPs, but the same is not true for inverted repeat (IR) and
 212 everted repeat (ER) motifs (A, D). The surprising correlation between MR motifs and deletion BPs is
 213 attenuated when MRs that have the same sequence as DR motifs are removed (B, C). Controls were
 214 generated by reshuffling the deletion BPs while maintaining their distribution (n=20, mean \pm SD shown).
 215 The schematic drawings above (A, D) depict the orientation of the repeat (XR) half-sites in relation to the
 216 BPs. *** p < 0.001; ** p < 0.01 by one sample t-test.

217

218 A) The number of deletions associated with DR, MR, IR or ER motifs at both BPs compared with
 219 reshuffled controls.

220 B) Venn diagram showing the number of MR, DR and hybrid MR-DR motifs that were identified within
 221 the major arc.

222 C) The number of deletions associated with MR motifs, before (MR) and after removal of hybrid MR-DR
 223 motifs (MR^{DR-}), compared with reshuffled controls.

224 D) The number of deletions associated with DR, MR, IR or ER motifs at either BP compared with
 225 reshuffled controls.

226

227 Predicted triplex-forming motifs are over-represented at mtDNA breakpoints

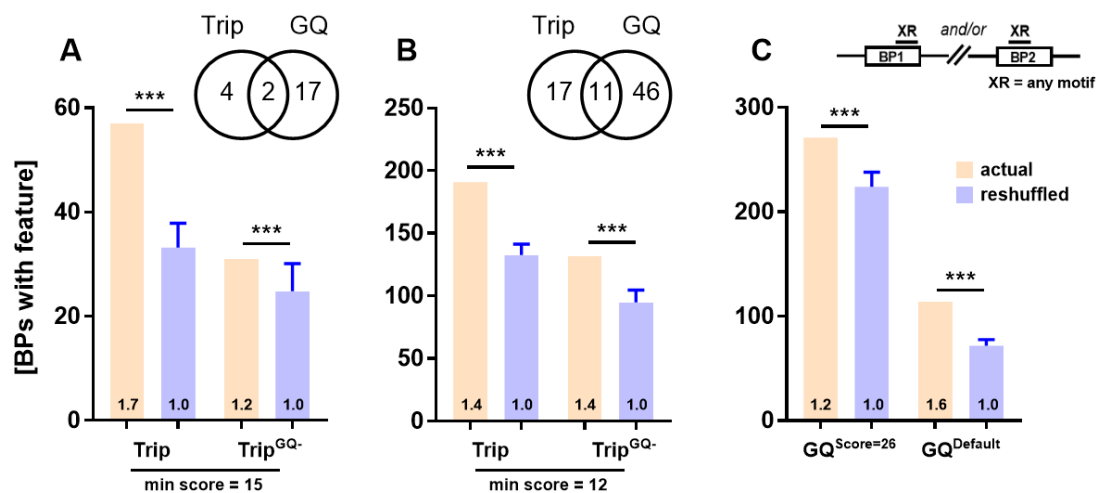
228 Given the association between MR motifs and breakpoints we decided to analyze triplex motifs, a
 229 special case of homopurine and homopyrimidine mirror repeats (Khristich and Mirkin 2020, Bissler
 230 2007), and their association with deletion breakpoints in the MitoBreak database.

231 Here, we use the triplex package to predict intramolecular triplex motifs because it has several
 232 advantages compared to other software (Hon et al. 2013). For example, using the nBMST tool, as in a
 233 previous study of mtDNA instability (Oliveira et al. 2013), we only identified two potential triplex motifs
 234 within the major arc that did not overlap with the six motifs identified by the triplex package (Table S1).
 235 In contrast, using Triplexator (Buske et al. 2013) we were able to detect four of the six triplex motifs and
 236 the motifs detected by Triplexator were also enriched at breakpoints (Table S2).

237 We noticed that predicted triplexes are G-rich and thus could be related to G-quadruplex motifs (Doluca
 238 et al. 2013). In a comparison of the two motif types, however, we found several differences (Table S1,
 239 S3). Triplex motifs were shorter and less abundant than predicted G-quadruplexes, associated with
 240 fewer breakpoints altogether (Fig. 3) and, in contrast to G-quadruplexes almost exclusive to the G-rich
 241 mtDNA heavy-strand, triplex motifs were also common on the light-strand.

242 The six triplex motifs detected by the triplex package were significantly enriched around deletion
 243 breakpoints and when we excluded triplex-G-quadruplex hybrid motifs the result was attenuated but
 244 remained significant (Fig. 3A). Given the higher risk of spurious findings with only six motifs, we
 245 repeated the analysis using a relaxed definition of triplex and the results were fundamentally unchanged
 246 (Fig. 3B). Furthermore, our results were not sensitive to reasonable changes in the size of the search
 247 window around breakpoints (Fig. S5A, B), motif quality scores (Fig. S5C, D) or inclusion of overlapping
 248 motifs (Fig. S5E-G).

249 Analogous to the situation with MR motifs we tested if overlapping triplex-DR hybrid motifs could bias
 250 our results. Given the rarity of triplex motifs and the many DRs in the mitochondrial genome we choose
 251 an alternative approach rather than excluding triplex motifs that overlapped any DR half-site. We
 252 compared the fraction of triplex and G-quadruplex positive deletions associated with DRs (GQ⁺, DR⁺ and
 253 Trip⁺, DR⁺) and not associated with DRs (GQ⁻, DR⁻ and Trip⁻, DR⁻). We considered a deletion to be DR⁺ if
 254 both breakpoints were flanked by the same DR sequence. In this case, only 44% of Trip⁺ deletions
 255 associated with DRs whereas 66% of GQ⁺ deletions did (Table S4).



256
 257 **Figure 3**

258 Triplex motifs are significantly enriched around actual breakpoints (BPs) compared to reshuffled BPs (A,
 259 B) even after removal of G-quadruplex (GQ)-triplex hybrid motifs (Trip^{GQ-}). The number of unique triplex

260 motifs, GQ motifs and of hybrid triplex-GQ motifs, within the mtDNA major arc, is shown in the Venn
261 diagrams above (A, B). Enrichment of GQ motifs around BPs is shown for comparison in (C). Controls
262 were generated by reshuffling the deletion BPs while maintaining their distribution (n=20, mean \pm SD
263 shown). The schematic drawing above (C) depicts the orientation of the GQ and triplex motifs (XR) in
264 relation to the BPs. *** $p < 0.0001$ by one sample t-test.

265

266 A) The number of deletion BPs associated with triplex motifs compared with reshuffled controls.
267 Analysis including (left side) or excluding triplex-GQ hybrid motifs (right side).

268 B) Same as (A) but with relaxed criteria for the detection of triplex motifs (min score=12) and GQ motifs
269 (min score=26).

270 C) The number of deletion BPs associated with GQ motifs compared with reshuffled controls. Relaxed
271 settings (left side, min score=26) and default settings (right side, min score=47).

272

273 **Triplex forming motifs may be associated with mitochondrial disease breakpoints**

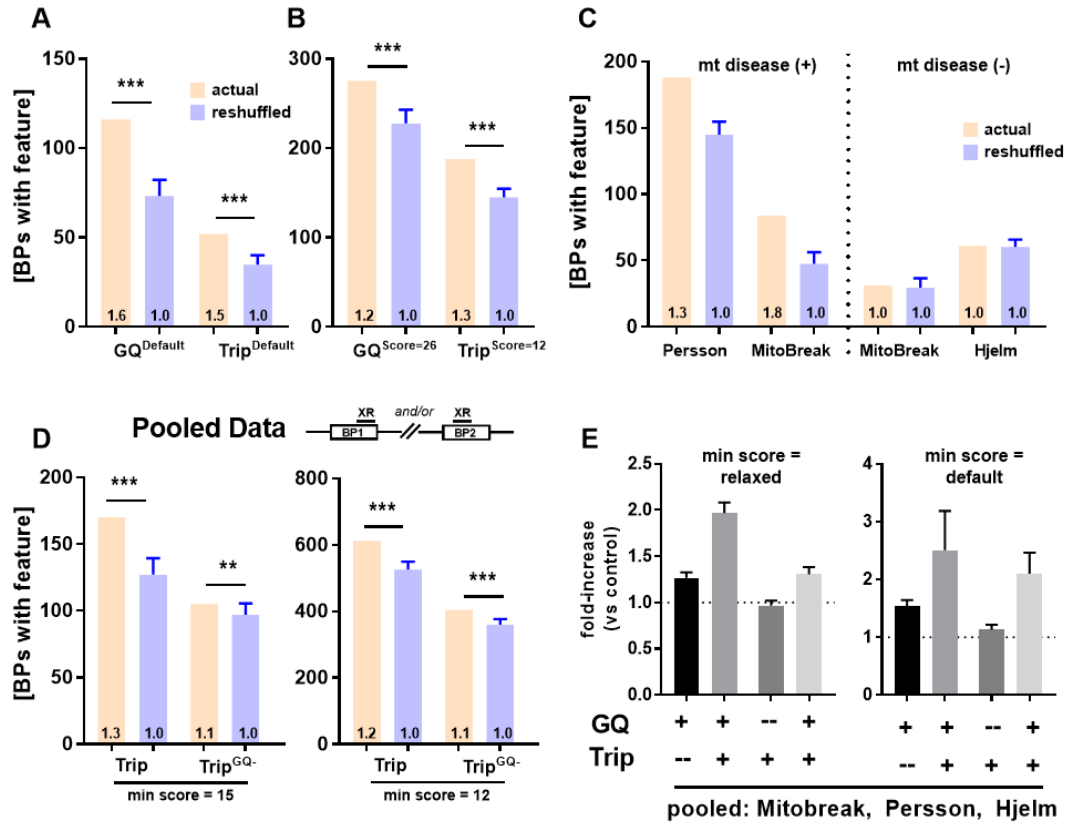
274 Next, we sought to validate our findings on two recently published next generation sequencing datasets
275 (Hjelm et al. 2019, Persson et al. 2019; **mtDNA Breakpoints.xlsx**; **Table S5**). We were able to confirm
276 the enrichment of DR (**Fig. S6A, S7A**), MR (**Fig. S6A, S7A**) and G-quadruplex motifs (**Fig. 4A, B; S6C, D**)
277 around deletion breakpoints. Additionally, we confirmed that hybrid MR-DR motifs are responsible in
278 large part for the enrichment of MR motifs around breakpoints (**Fig. S6B, S7B**).

279 In contrast, we found that triplex motifs were not consistently enriched around breakpoints in the
280 dataset of Hjelm et al. (**Fig. S6C, D**), which is based on post-mortem brain samples from patients without
281 overt mitochondrial disease, whereas we saw enrichment in the dataset by Persson et al. (**Fig. 4A, B**),
282 which is based on muscle biopsies from patients with mitochondrial disease. This unexpected
283 discrepancy prompted us to take a second look at the MitoBreak data. In this dataset triplex motifs were
284 significantly more enriched at breakpoints in the mtDNA single deletion subgroup compared to the
285 healthy tissues subgroup (**Fig. S8**). In addition, we found more broadly that mitochondrial disease status
286 might explain the heterogenous results across datasets we have seen (**Fig. 4C**).

287 Further strengthening our findings, triplex motifs were enriched in the MitoBreak and Persson et al.
288 dataset regardless of the breakpoint shuffling method chosen and of our statistical assumptions (**Fig.**
289 **S9**). What is more, triplex motifs were also enriched at breakpoints when we pooled all three datasets
290 (**Fig. 4D**), although to a lesser extent.

291 Finally, G-quadruplex motifs close to triplex motifs were more strongly enriched at deletion breakpoints
292 than solitary G-quadruplex motifs (**Fig. 4E; Fig. S10**), suggesting that triplex formation may further
293 contribute to DNA instability.

294



295
296

Figure 4

297 In the **Persson et al. (2019)** dataset, triplex and G-quadruplex (GQ) motifs are enriched around deletion
298 breakpoints (BPs), using either default (A) or relaxed scoring criteria (B). Although triplex motifs
299 predominate in mitochondrial disease datasets (C), we also find that triplex motifs are significantly
300 enriched around BPs (D) after pooling the data from **MitoBreak, Persson et al. (2019) and Hjelm et al**
301 **(2019)**. Finally, GQ and triplex motifs show stronger enrichment around BPs than either of them in
302 isolation (E). Controls were generated by reshuffling the deletion BPs while maintaining their
303 distribution (n=20, mean \pm SD shown). The schematic drawing above (D) depicts the orientation of the
304 motifs (XR) in relation to the BPs. *** p<0.0001, **p<0.001 by one sample t-test.

305

306 A) The number of deletion BPs associated with GQ and triplex motifs compared with reshuffled controls
307 (min score = default).

308 B) The number of deletion BPs associated with GQ and triplex motifs compared with reshuffled controls
309 (min score = relaxed).

310 C) The number of deletion BPs associated with triplex motifs (relaxed settings, min score=12) stratified
311 by mitochondrial disease status. MitoBreak data includes single and multiple mitochondrial deletion
312 syndromes.

313 D) The number of deletion BPs associated with triplex motifs, or with triplex motifs excluding triplex-GQ
314 hybrid motifs (Trip^{GQ-}), compared with reshuffled controls. Default settings (left side, min score=15) and
315 relaxed settings (right side, min score=12).

316 E) The fold-enrichment of GQ and triplex motifs around deletion BPs is shown. Motifs were considered
317 overlapping if their midpoints were within 50 bp.

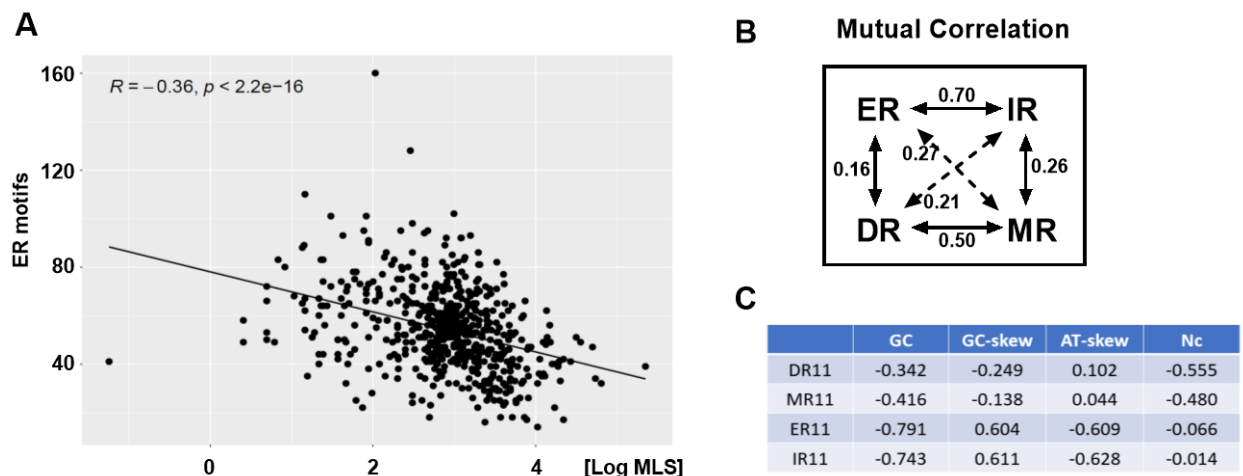
318

319 **Repeats and lifespan: no support for the theory of resistant biomolecules**

320 For our analysis, we focus on 11 bp long repeat motifs as short repeats are less likely to allow stable
 321 base pairing and longer repeats are rare (**Fig. S11**) and because results considering repeat motifs of
 322 different lengths usually agree with each other (**Table S6**; **Yang et al. 2013**). To allow comparability with
 323 other studies (**Lakshmanan et al. 2015**) we analyzed non D-loop motifs, but results for major arc motifs
 324 are numerically similar (**Table S7**).

325 First, consistent with **Yang et al. (2013)** we found that IR motifs show a negative correlation with the
 326 MLS of mammals in the unadjusted model. In addition, we identified ER motifs, a class of symmetrically
 327 related repeats, that show an even stronger inverse relationship with longevity (**Fig. 5A**; **Table 1**).
 328 However, these inverse correlations vanished after taking into account body mass, base composition
 329 and phylogeny in a PGLS model (**Table 1**). Second, in agreement with **Lakshmanan et al. (2015)** we
 330 found that DR motifs do not correlate with the MLS of mammals. The same was true for the
 331 symmetrically related MR motifs. Just as with IR motifs, modest inverse correlations vanished in the fully
 332 adjusted model (**Table 1**). We also found the same null results in two other vertebrate classes, birds and
 333 ray-finned fishes (**Table S6**). To gain hints as to causality, we finally tested if longer repeats, allowing
 334 more stable base pairing, show stronger correlations with MLS, but to our surprise we noticed the
 335 opposite (**Fig. S12A-D**).

336 Considering all four types of repeats together, we noticed that repeats with both half-sites on the same
 337 strand (DR and MR) or half-sites opposite strands (IR and ER) were correlated with each other (**Fig. 5B**)
 338 and with the same mtDNA compositional biases (**Fig. 5C**). Thus, for DR and MR motifs, an apparent
 339 relationship with MLS may be explained by their inverse relationship with GC content and for IR and ER
 340 motifs by an inverse relationship with GC content and a positive relationship with GC skew.



341

342 **Figure 5**

343 The number of everted repeat (ER) motifs is negatively correlated with species MLS in an unadjusted
 344 analysis (A). Repeats with a similar orientation correlate with each other (B). Direct repeat (DR) and
 345 mirror repeat (MR) motifs have a similar orientation since both half-sites are found on the same strand
 346 and in the case of ER and inverted repeat (IR) motifs the half-sites are on opposite strands. Finally, we
 347 show the major mtDNA compositional biases that co-vary with the four repeat classes (C) and may

348 explain an apparent correlation with MLS. Data is for 11 bp long repeats and Pearson's R is shown in (A-
349 C).

350

351 **Table 1. Correlation between potentially mutagenic motifs and species lifespan**

Motif	Type	Raw	Adjusted
DR11	11bp	<u>-0.113</u>	0.055
MR11	11bp	<u>-0.155</u>	-0.002
IR11	11bp	<u>-0.336</u>	<u>0.105</u>
ER11	11bp	<u>-0.356</u>	-0.047
triplex	default	<u>-0.296</u>	<u>-0.211**</u>
triplex	relaxed	<u>-0.190</u>	<u>-0.127^</u>
GQ	default	<u>0.264</u>	0.068
GQ	relaxed	<u>0.283</u>	-0.097**

352 The adjusted model takes into account body mass, GC content, GC skew, AT skew and number of
353 effective codons. Significant correlations in the raw or adjusted model are bolded/underlined ($p < 0.05$).
354 The PGLS model additionally considers phylogeny. ^denotes p-values of $0.05 < p < 0.10$ in the PGLS model
355 and ** p-values of $p < 0.05$. The table shows Pearson's R.

356 **Triplex motifs, not G-quadruplexes, show an inverse relationship with species lifespan**

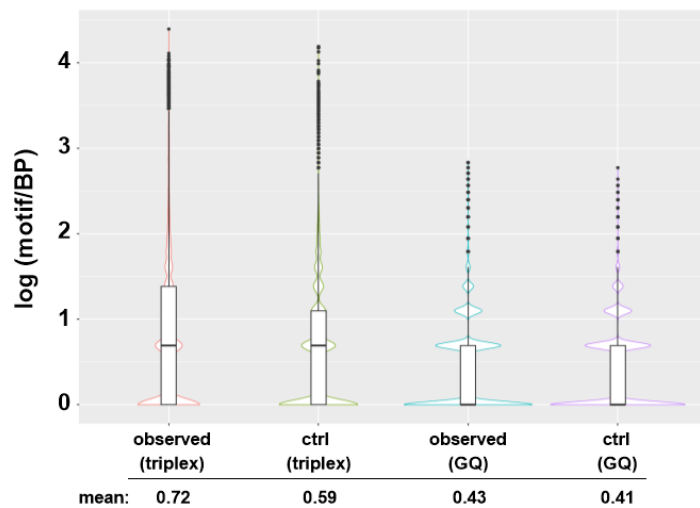
357 So far, no survey of G-quadruplex and triplex motifs has been conducted across species, although it is
358 known that human mtDNA contains more G-quadruplexes than mouse, rat or monkey mtDNA (**Bharti et**
359 **al. 2014**). First, we confirmed that different tools to detect G-quadruplex motifs agree with each other
360 (**Lombardi and Londoño-Vallejo 2020; Fig. S13**). The results of different triplex detection tools,
361 however, were inconsistent. While we were able to detect some overlap between the motifs found with
362 Triplexator and the triplex package in human mtDNA (**Table S1**), we found that the two tools made very
363 different predictions regarding triplex counts across species (**Fig. S14**).

364 The limited agreement between publicly available triplex detection tools raised the question whether
365 our preferred tool, the triplex package in R, detects the same class of mutagenic triplex motifs as
366 reported in earlier studies using in-house scripts (**Bacolla et al. 2016**). To answer this question, we
367 reanalyzed a large dataset of over 500000 cancer associated breakpoints. In line with this earlier study,
368 we found that both triplex and G-quadruplex motifs were significantly enriched around actual
369 breakpoints compared to control breakpoints (**Fig. 6; Table S8**) and that breakpoints were preferably
370 found in highly unstable regions with multiple such motifs (**Fig. S15**).

371 Next, we turned again to mtDNA to test whether mutagenic motifs are negatively correlated with MLS
372 as predicted by the theory of resistant biomolecules. To the contrary, we found that G-quadruplex
373 motifs were positively correlated with MLS (**Fig. S16**), although this may be secondary to their strong
374 correlation with GC content. However, even after taking into account base composition and phylogeny
375 using PGLS there was no convincing relationship between G-quadruplex motifs and MLS (**Table 1**).

376 In contrast, we found a moderate, negative correlation between intramolecular triplex motifs and the
377 MLS of mammals (**Fig. 7A**) that was significant after correcting for body mass and base composition and,
378 for triplex motifs using default scoring, also after correction for phylogeny using PGLS (**Table 1**). This
379 result remained stable when we varied the score-cutoff and in fact triplexes were the only motif class
380 for which we found that higher confidence motifs, i.e. motifs predicted to be more stable, showed a
381 stronger relationship with MLS (**Fig. S12E**).

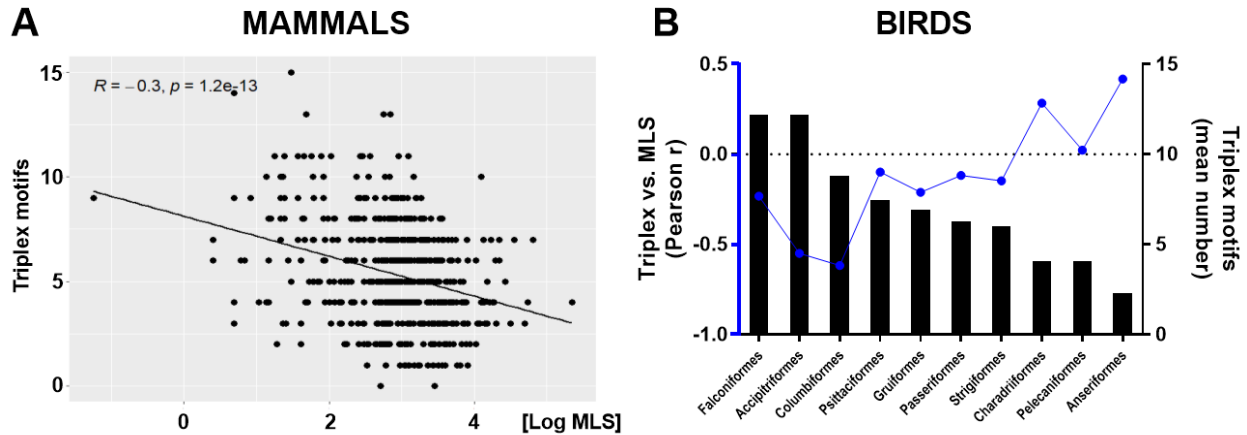
382 Although we found no significant relationship between triplex motifs and MLS of birds or ray-finned
383 fishes, we noticed that this finding was modulated by the number of triplex motifs in the mtDNA of birds
384 (**Fig. 7B**) and mammals (**Fig. S17B, D**). Phylogenetic orders with higher numbers of triplex motifs in their
385 mtDNA showed a stronger inverse relationship between MLS and triplex counts than orders with few
386 such motifs. Thus, when we split the bird and mammal data into orders with mitochondrial triplex levels
387 above or below the median, we found a significant inverse relationship between MLS and triplex motifs
388 in the high group for both birds and mammals (**Table S9**).



389
390 **Figure 6**

391 Actual cancer-related breakpoints (BPs) are associated with more triplex and G-quadruplex (GQ) motifs
392 compared to control BPs ($p < 2.2e-16$; Wilcoxon rank sum test). To allow better visualization of the data,
393 the number of motifs for each BP was log-transformed and $\log(0)$ values were excluded. Box whisker
394 plots show the median, interquartile range and outliers while the underlying violin plot shows the actual
395 distribution.

396



397
398

Figure 7

399 Across mammals, mitochondrial triplex motifs are inversely correlated with maximum lifespan (MLS) in
400 an unadjusted analysis (A). Although, birds do not show a correlation between triplex motifs and MLS in
401 the whole dataset (**Table S6**), the correlations between triplex motifs and MLS are stronger in bird
402 orders with higher mean triplex levels (B).

403 A) Mammals with a higher number of triplex motifs in their mtDNA (default settings) are on average
404 shorter-lived.

405 B) The higher the mean number of triplex motifs in a bird order (bar graphs) the stronger the inverse
406 correlation between triplex motifs and MLS in the same order (blue line). All bird orders with more than
407 5 species in our dataset are included in this graph.

408

DISCUSSION

Repeat motifs and mtDNA deletions

411 Our goal was to define motifs associated with mtDNA deletions that would be then expected to show an
412 inverse correlation with MLS under the theory of resistant biomolecules. We found that DR, MR, G-
413 quadruplex and triplex motifs would be plausible candidates.

414 Specifically, our results support the consensus that DR and G-quadruplex motifs are major drivers of
415 deletion mutagenesis (**Persson et al. 2019**) but not IR motifs (**Dong et al. 2014**; but see also: **Damas et**
416 **al. 2012**, **Mikhailova et al. 2020**). In addition, we found a novel association between MR motifs and
417 mtDNA deletions (**Fig. 2A**). This was unexpected since MR motifs do not allow for canonical base-pairing.
418 Nonetheless, some studies have found MR motifs to be associated with indels (**Georgakopoulos-Soares**
419 **et al. 2018**), perhaps due to their ability to form triplex DNA (**Kamat et al. 2016**).

420 Triplex forming motifs are mutagenic in bacteria (**Holder et al. 2015**), associated with deletions and
421 translocations in cancer (**Bacolla et al. 2016**) and with mutations underlying various inherited diseases
422 (**Kamat et al. 2016**), but little was known about their role in mitochondria. This is the first report that
423 mitochondrial triplex motifs are indeed associated with mtDNA deletions (**Fig. 3**) and MLS (**Fig. 7**).

Some mtDNA motifs colocalize and may interact

425 One key finding that emerged during our analysis was that motif classes correlate with each other, e.g.,

426 if both classes are enriched in DNA regions with a biased composition. Mitochondrial DR motifs are
427 often close to MR and G-quadruplex motifs (**Fig. S18, Table S4**), IR motifs to ER motifs (**Table S10**) and
428 triplex motifs to G-quadruplex motifs (**Fig. 3**). Our work is a first attempt to disentangle these
429 interactions both in relation to deletion formation and to lifespan.

430 In principle one can correct for this by excluding hybrid motifs, i.e. two motifs located close to each
431 other, from the analysis, as we have done in **Fig. 2-4**, but it is not always clear whether this is biologically
432 sensible or overly conservative.

433 In the case of MR repeats we are inclined to conclude that they do not contribute to mtDNA instability,
434 since there is little experimental data to implicate non-triplex-forming MRs in DNA instability and the
435 enrichment of MR motifs at deletion breakpoints is attenuated after we exclude MR-DR hybrid motifs
436 from the analysis (**Fig. 2C; Fig. S6, S7**).

437 In contrast, both triplex and G-quadruplex motifs are strongly implicated in DNA instability. A high G-
438 content is known to promote G-quadruplex formation and to stabilize triplex DNA (**Buske et al. 2011,**
439 **Kaufmann et al. 2019**) thus explaining their colocalization. Although G-quadruplexes may compete with
440 the formation of triplex DNA, this is not always so (**Solé et al. 2017, del Mundo et al. 2017**).
441 Furthermore, in mtDNA, where overlapping triplex and G-quadruplex motifs can be located on opposite
442 strands, a secondary structure on one strand could potentially promote formation of a secondary
443 structure on the other strand by preventing reannealing of the two strands, as has been suggested for R-
444 loops that promote the formation of G-quadruplexes (**De Magis et al. 2019**).

445 In support of the idea that motifs can interact, we found that G-quadruplex and triplex motifs in
446 proximity to each other showed stronger associations with deletion breakpoints than isolated motifs,
447 suggesting that their effects are additive (**Fig. S10**).

448 Similarly, it is not clear if the enrichment of G-quadruplex motifs at mtDNA deletion breakpoints needs
449 to be corrected for their proximity to DR motifs (**Table S4**) found in regions of high GC-skew (**Fig. S18**). In
450 a preliminary analysis we found that removal of DR-G-quadruplex hybrid sequences can greatly
451 attenuate the over-representation of G-quadruplex motifs around breakpoints (data not shown). A
452 thorough re-analysis of this phenomenon is beyond the scope of this work, but it does suggest that
453 colocalization of different motifs is not a problem unique to our triplex dataset.

454 **mtDNA motifs in health and disease**

455 We found that triplex motifs were particularly enriched around breakpoints in datasets from patients
456 with mitochondrial disease (**Fig. 4C**). Conceivably, polymerase stalling associated with mitochondrial
457 disease (**Wanrooij and Falkenberg 2010**) could allow more time for the formation of triplex DNA during
458 replication, thereby explaining this finding. Consistent with this idea, a preprint by **Lakshmanan et al.**
459 **(2018)** showed that mtDNA deletions in patients with mitochondrial disease due to POLG mutations are
460 explained by predominantly short repeats and this bias towards short repeats was recently confirmed by
461 a larger analysis that compared POLG patients to healthy controls (**Lujan et al. 2020**). These findings are
462 intriguing because medium and long repeats are preferably associated with strand-slippage mechanisms
463 whereas short repeats are consistent with strand breaks (**Nissanka et al. 2019, Lakshmanan et al. 2018**)
464 which can be caused by ROS or secondary structures like G-quadruplex and triplex motifs.

465 **Analysis of mutagenic motifs and their relationship with lifespan casts doubt on the theory of**
466 **resistant biomolecules**

467 The theory of resistant biomolecules can be seen to imply a correlation between mutagenic motifs and
468 MLS, but despite promising data from earlier studies (**Lakshmanan et al. 2012, Yang et al. 2013**), we
469 found that neither G-quadruplex, DR, MR, IR nor ER motifs were associated with MLS after correcting for
470 phylogeny and base composition (**Table 1**).

471 Perhaps the mtDNA is too streamlined to allow for the necessary changes in sequence. Given thousands
472 of short, potentially mutagenic motifs (**Fig. S11**) that would need to be lost, we speculate it is more likely
473 that nuclear proteins involved in mtDNA maintenance and metabolism account for the different rates of
474 age-related deletion accumulation across species (**Guo et al. 2010**). In fact, repeats enable error prone
475 DNA repair (**Tadi et al. 2016**), which might be advantageous under genotoxic stress to prevent
476 wholesale mtDNA degradation and only detrimental late in life due to deletion accumulation, as would
477 be predicted by the theory of antagonistic pleiotropy (**Campisi and Vijg 2009**).

478 The literature appears largely consistent with the null hypothesis. The work by **Yang et al. (2013)** may be
479 considered the strongest case in favor of resistant biomolecules. They found an inverse relationship
480 between IR motifs and MLS after correcting for phylogeny only. We found a similar correlation which,
481 however, is fully accounted for by base composition. Two other findings of their paper are also
482 consistent with the null hypothesis. Longer IR motifs, presumably allowing more stable base pairing, did
483 not show a stronger inverse correlation with MLS, which we confirmed (**Fig. S12C**). Secondly, IR motifs
484 with half-sites close together failed to show a stronger relationship with MLS, although these should
485 form secondary structures more easily.

486 **The importance of mtDNA base composition in motif-lifespan correlations**

487 It is striking that most of the findings were attenuated when we controlled for the base composition of
488 mtDNA. Although the importance of such an adjustment was already highlighted by **Lakshmanan et al.**
489 (**2015**) for DR motifs, we are the first to apply these corrections in the study of multiple DNA motifs.

490 We find it particularly informative to consider related motif classes together (**Fig. 5B, C**). ER motifs, for
491 example, just like IR motifs show a strong correlation with GC content and GC skew, which in turn
492 correlate with MLS. Importantly, ER motifs were not associated with mtDNA deletion breakpoints (**Fig.**
493 **2A, D**), are not known to be mutagenic, do not permit canonical base pairing and yet show a stronger
494 inverse correlation with MLS than do IR motifs, which is fully attenuated after adjustment for base
495 composition (**Table 1**). Thus, we conclude that most earlier results were driven by compositional bias.

496 **Can triplex motifs save the theory of resistant biomolecules?**

497 We showed that intramolecular triplex motifs detected by the triplex package are inversely correlated
498 with mammalian MLS after correcting for body mass, base composition and phylogeny (**Table 1**).
499 Although this moderate inverse correlation with MLS provides some support for this theory, it is not
500 clear why major arc triplex motifs show a weaker than expected correlation with MLS (**Table S7**) nor if
501 the triplex data can be generalized to non-mammalian species.

502 While we do not know a priori which motifs might be mutagenic in species with different mtDNA
503 biology, we did find preliminary evidence that triplex motifs are inversely correlated with MLS in bird
504 orders with high numbers of triplex motifs in their mtDNA (**Fig. 7B**) but no such correlation in ray-finned
505 fishes. Since we observed the same trend in mammals, this suggests a potential threshold effect.

506 Perhaps a small number of triplex motifs in mtDNA is well tolerated, whereas larger numbers are
507 progressively more destabilizing, especially if they occur in clusters as demonstrated for nuclear triplex
508 motifs (**Fig. S15**).

509 **Going forward, finding the right motifs?**

510 Why did an earlier study (**Oliveira et al. 2013**) fail to uncover an association between triplex motifs and
511 mtDNA deletions? According to **Hon et al. (2013)** the nBMST tool used in that study only detects triplex-
512 like mirror repeats and we also found it to be not very sensitive for the detection of putative triplex
513 sequences. Given these shortcomings we also tested two other tools. The first one was Triplexator,
514 which detects triplex target and triplex forming sites that could form both intra- and intermolecular
515 triplexes, and the second one was the triplex package that detects intramolecular triplexes. We
516 reasoned that intramolecular triplexes would be the most stable thus settling to use the latter tool.
517 Using the triplex package we were able to confirm the well-established finding that nuclear triplex
518 motifs are found near cancer-related breakpoints, supporting the validity of this tool (**Table S8**).

519 Although some of the sequences detected with Triplexator and the triplex package overlapped, many
520 did not and in a comparison of 600 mammalian species the numbers of detected motifs did not
521 correlate between the two tools (**Fig. S14**). This highlights a broader issue about the selection of motif
522 detection tools. While multiple mature G-quadruplex detection tools exist that tend to agree with each
523 other (**Fig. S13; Lombardi and Londoño-Vallejo 2020**), the choices for triplex motifs are more limited
524 and there is little in vivo validation in mammalian genomes (**Kaufmann et al. 2019**).

525 Given these uncertainties, perhaps going forward we can refine the search parameters to find motifs
526 that show a stronger correlation with lifespan and mtDNA deletions. To this end, our analysis of
527 mitochondrial and nuclear breakpoints raises the possibility that hybrid and clustered motifs are
528 particularly harmful (**Fig. 4E; Fig. S15**), but we have not yet analyzed these across genomes. Another
529 issue that we did not address in detail is the type and orientation of triplex motifs involved in mtDNA
530 deletions. Most importantly, future studies should explore to what extent these predicted
531 intramolecular triplexes form in mitochondria.

532 **ACKNOWLEDGEMENTS**

533 We thank Doug Turnbull, Amy Vincent, David Meyer and Teresa Valencak for helpful comments and/or
534 support. Reginald Smith for providing the python code to calculate Wright's Nc, Mitya Toren for sharing
535 updated MitoAge data and John A. Tainer for sharing triplex-related data.

536 **REFERENCES**

537 Aledo, J. C., Valverde, H., & de Magalhães, J. P. (2012). Mutational Bias Plays an Important Role in Shaping
538 Longevity-Related Amino Acid Content in Mammalian mtDNA-Encoded Proteins. *Journal of Molecular*
539 *Evolution*, 74(5–6), 332–341. <https://doi.org/10.1007/s00239-012-9510-7>

540 Bacolla, A., Tainer, J. A., Vasquez, K. M., & Cooper, D. N. (2016). Translocation and deletion breakpoints in
541 cancer genomes are associated with potential non-B DNA-forming sequences. *Nucleic Acids Research*,
542 44(12), 5673–5688. <https://doi.org/10.1093/nar/gkw261>

543 Bender, A., Krishnan, K. J., Morris, C. M., Taylor, G. A., Reeve, A. K., Perry, R. H., Jaros, E., Hersheson, J. S.,
544 Betts, J., Klopstock, T., Taylor, R. W., & Turnbull, D. M. (2006). High levels of mitochondrial DNA deletions

- 545 in substantia nigra neurons in aging and Parkinson disease. *Nature Genetics*, 38(5), 515–517.
546 <https://doi.org/10.1038/ng1769>
- 547 Bharti, S. K., Sommers, J. A., Zhou, J., Kaplan, D. L., Spelbrink, J. N., Mergny, J.-L., & Brosh, R. M. (2014).
548 DNA Sequences Proximal to Human Mitochondrial DNA Deletion Breakpoints Prevalent in Human Disease
549 Form G-quadruplexes, a Class of DNA Structures Inefficiently Unwound by the Mitochondrial Replicative
550 Twinkle Helicase. *Journal of Biological Chemistry*, 289(43), 29975–29993.
551 <https://doi.org/10.1074/jbc.M114.567073>
- 552 Bissler, J. J. (2007). Triplex DNA and human disease. *Frontiers in Bioscience: A Journal and Virtual Library*,
553 12, 4536–4546. <https://doi.org/10.2741/2408>
- 554 Buske, F. A., Bauer, D. C., Mattick, J. S., & Bailey, T. L. (2013). Triplex-Inspector: An analysis tool for triplex-
555 mediated targeting of genomic loci. *Bioinformatics*, 29(15), 1895–1897.
556 <https://doi.org/10.1093/bioinformatics/btt315>
- 557 Buske, F. A., Mattick, J. S., & Bailey, T. L. (2011). Potential in vivo roles of nucleic acid triple-helices. *RNA*
558 *Biology*, 8(3), 427–439. <https://doi.org/10.4161/rna.8.3.14999>
- 559 Butler, T. J., Estep, K. N., Sommers, J. A., Maul, R. W., Moore, A. Z., Bandinelli, S., Cucca, F., Tuke, M. A.,
560 Wood, A. R., Bharti, S. K., Bogenhagen, D. F., Yakubovskaya, E., Garcia-Diaz, M., Guillian, T. A., Byrd, A. K.,
561 Raney, K. D., Doherty, A. J., Ferrucci, L., Schlessinger, D., ... Brosh, R. M. (2020). Mitochondrial genetic
562 variation is enriched in G-quadruplex regions that stall DNA synthesis in vitro. *Human Molecular Genetics*,
563 29(8), 1292–1309. <https://doi.org/10.1093/hmg/ddaa043>
- 564 Campisi, J., & Vijg, J. (2009). Does Damage to DNA and Other Macromolecules Play a Role in Aging? If So,
565 How? *The Journals of Gerontology: Series A*, 64A(2), 175–178. <https://doi.org/10.1093/gerona/gln065>
- 566 Cer, R. Z., Bruce, K. H., Donohue, D. E., Temiz, A. N., Bacolla, A., Mudunuri, U. S., Yi, M., Volfovsky, N.,
567 Luke, B. T., Collins, J. R., & Stephens, R. M. (2011). Introducing the non-B DNA Motif Search Tool (nBMST).
568 *Genome Biology*, 12(1), P34. <https://doi.org/10.1186/1465-6906-12-S1-P34>
- 569 Damas, J., Carneiro, J., Amorim, A., & Pereira, F. (2014). MitoBreak: The mitochondrial DNA breakpoints
570 database. *Nucleic Acids Research*, 42(D1), D1261–D1268. <https://doi.org/10.1093/nar/gkt982>
- 571 Damas, J., Carneiro, J., Gonçalves, J., Stewart, J. B., Samuels, D. C., Amorim, A., & Pereira, F. (2012).
572 Mitochondrial DNA deletions are associated with non-B DNA conformations. *Nucleic Acids Research*,
573 40(16), 7606–7621. <https://doi.org/10.1093/nar/gks500>
- 574 del Mundo, I. M. A., Zewail-Foote, M., Kerwin, S. M., & Vasquez, K. M. (2017). Alternative DNA structure
575 formation in the mutagenic human c-MYC promoter. *Nucleic Acids Research*, 45(8), 4929–4943.
576 <https://doi.org/10.1093/nar/gkx100>
- 577 Doluca, O., Withers, J. M., & Filichev, V. V. (2013). Molecular Engineering of Guanine-Rich Sequences: Z-
578 DNA, DNA Triplexes, and G-Quadruplexes. *Chemical Reviews*, 113(5), 3044–3083.
579 <https://doi.org/10.1021/cr300225q>
- 580 Dong, D. W., Pereira, F., Barrett, S. P., Kolesar, J. E., Cao, K., Damas, J., Yatsunyk, L. A., Johnson, F. B., &
581 Kaufman, B. A. (2014). Association of G-quadruplex forming sequences with human mtDNA deletion
582 breakpoints. *BMC Genomics*, 15(1), 677. <https://doi.org/10.1186/1471-2164-15-677>

- 583 Gammage, P. A., Rorbach, J., Vincent, A. I., Rebar, E. J., & Minczuk, M. (2014). Mitochondrially targeted
584 ZFNs for selective degradation of pathogenic mitochondrial genomes bearing large-scale deletions or
585 point mutations. *EMBO Molecular Medicine*, 6(4), 458–466. <https://doi.org/10.1002/emmm.201303672>
- 586 Georgakopoulos-Soares, I., Morganella, S., Jain, N., Hemberg, M., & Nik-Zainal, S. (2018). Noncanonical
587 secondary structures arising from non-B DNA motifs are determinants of mutagenesis. *Genome Research*,
588 28(9), 1264–1271. <https://doi.org/10.1101/gr.231688.117>
- 589 Gladyshev, V. N. (2013). The Free Radical Theory of Aging Is Dead. Long Live the Damage Theory!
590 *Antioxidants & Redox Signaling*, 20(4), 727–731. <https://doi.org/10.1089/ars.2013.5228>
- 591 Guo, X., Kudryavtseva, E., Bodyak, N., Nicholas, A., Dombrovsky, I., Yang, D., Kraytsberg, Y., Simon, D. K., &
592 Khrapko, K. (2010). Mitochondrial DNA deletions in mice in men: Substantia nigra is much less affected in
593 the mouse. *Biochimica et Biophysica Acta (BBA) - Bioenergetics*, 1797(6), 1159–1162.
594 <https://doi.org/10.1016/j.bbabi.2010.04.005>
- 595 Gurusaran, M., Ravella, D., & Sekar, K. (2013). RepEx: Repeat extractor for biological sequences.
596 *Genomics*, 102(4), 403–408. <https://doi.org/10.1016/j.ygeno.2013.07.005>
- 597 Hamilton, K. L., & Miller, B. F. (2016). What is the evidence for stress resistance and slowed aging?
598 *Experimental Gerontology*, 82, 67–72. <https://doi.org/10.1016/j.exger.2016.06.001>
- 599 Hjelm, B. E., Rollins, B., Morgan, L., Sequeira, A., Mamdani, F., Pereira, F., Damas, J., Webb, M. G., Weber,
600 M. D., Schatzberg, A. F., Barchas, J. D., Lee, F. S., Akil, H., Watson, S. J., Myers, R. M., Chao, E. C., Kimonis,
601 V., Thompson, P. M., Bunney, W. E., & Vawter, M. P. (2019). Splice-Break: Exploiting an RNA-seq splice
602 junction algorithm to discover mitochondrial DNA deletion breakpoints and analyses of psychiatric
603 disorders. *Nucleic Acids Research*, 47(10), e59–e59. <https://doi.org/10.1093/nar/gkz164>
- 604 Holder, I. T., Wagner, S., Xiong, P., Sinn, M., Frickey, T., Meyer, A., & Hartig, J. S. (2015). Intrastrand triplex
605 DNA repeats in bacteria: A source of genomic instability. *Nucleic Acids Research*, 43(21), 10126–10142.
606 <https://doi.org/10.1093/nar/gkv1017>
- 607 Hon, J., Martínek, T., Rajdl, K., & Lexa, M. (2013). Triplex: An R/Bioconductor package for identification
608 and visualization of potential intramolecular triplex patterns in DNA sequences. *Bioinformatics*, 29(15),
609 1900–1901. <https://doi.org/10.1093/bioinformatics/btt299>
- 610 Hon, J., Martínek, T., Zendulka, J., & Lexa, M. (2017). pqsfinder: An exhaustive and imperfection-tolerant
611 search tool for potential quadruplex-forming sequences in R. *Bioinformatics*, 33(21), 3373–3379.
612 <https://doi.org/10.1093/bioinformatics/btx413>
- 613 Kamat, M. A., Bacolla, A., Cooper, D. N., & Chuzhanova, N. (2016). A Role for Non-B DNA Forming
614 Sequences in Mediating Microlesions Causing Human Inherited Disease. *Human Mutation*, 37(1), 65–73.
615 <https://doi.org/10.1002/humu.22917>
- 616 Kaufmann, B., Willinger, O., Eden, N., Kermas, L., Anavy, L., Solomon, O., Atar, O., Yakhini, Z., Goldberg, S.,
617 & Amit, R. (2019). Identifying triplex binding rules in vitro leads to creation of a new synthetic regulatory
618 tool in vivo. *BioRxiv*, 2019.12.25.888362. <https://doi.org/10.1101/2019.12.25.888362>
- 619 Kauppila, T. E. S., Kauppila, J. H. K., & Larsson, N.-G. (2017). Mammalian Mitochondria and Aging: An
620 Update. *Cell Metabolism*, 25(1), 57–71. <https://doi.org/10.1016/j.cmet.2016.09.017>

- 621 Khaidakov, M., Siegel, E. R., & Shmookler Reis, R. J. (2006). Direct repeats in mitochondrial DNA and
622 mammalian lifespan. *Mechanisms of Ageing and Development*, 127(10), 808–812.
623 <https://doi.org/10.1016/j.mad.2006.07.008>
- 624 Khrapko, K., Kraytsberg, Y., Grey, A. D. D., Vijg, J., & Schon, E. A. (2006). Does premature aging of the
625 mtDNA mutator mouse prove that mtDNA mutations are involved in natural aging? *Aging Cell*, 5(3), 279–
626 282. <https://doi.org/10.1111/j.1474-9726.2006.00209.x>
- 627 Khristich, A. N., & Mirkin, S. M. (2020). On the wrong DNA track: Molecular mechanisms of repeat-
628 mediated genome instability. *Journal of Biological Chemistry*, 295(13), 4134–4170.
629 <https://doi.org/10.1074/jbc.REV119.007678>
- 630 Lakshmanan, L. N., Gruber, J., Halliwell, B., & Gunawan, R. (2012). Role of Direct Repeat and Stem-Loop
631 Motifs in mtDNA Deletions: Cause or Coincidence? *PLoS ONE*, 7(4).
632 <https://doi.org/10.1371/journal.pone.0035271>
- 633 Lakshmanan, L. N., Gruber, J., Halliwell, B., & Gunawan, R. (2015). Are mutagenic non D-loop direct repeat
634 motifs in mitochondrial DNA under a negative selection pressure? *Nucleic Acids Research*, 43(8), 4098–
635 4108. <https://doi.org/10.1093/nar/gkv299>
- 636 Lakshmanan, L. N., Yee, Z., Gruber, J., Halliwell, B., & Gunawan, R. (2018). Thermodynamic analysis of
637 mitochondrial DNA breakpoints reveals mechanistic details of deletion mutagenesis [Preprint]. *Systems*
638 *Biology*. <https://doi.org/10.1101/254631>
- 639 Lawless, C., Greaves, L., Reeve, A. K., Turnbull, D. M., & Vincent, A. E. (2020). The rise and rise of
640 mitochondrial DNA mutations. *Open Biology*, 10(5), 200061. <https://doi.org/10.1098/rsob.200061>
- 641 Lujan, S. A., Longley, M. J., Humble, M. H., Lavender, C. A., Burkholder, A., Blakely, E. L., Alston, C. L.,
642 Gorman, G. S., Turnbull, D. M., McFarland, R., Taylor, R. W., Kunkel, T. A., & Copeland, W. C. (2020).
643 Ultrasensitive deletion detection links mitochondrial DNA replication, disease, and aging. *Genome*
644 *Biology*, 21(1), 248. <https://doi.org/10.1186/s13059-020-02138-5>
- 645 Magis, A. D., Manzo, S. G., Russo, M., Marinello, J., Morigi, R., Sordet, O., & Capranico, G. (2019). DNA
646 damage and genome instability by G-quadruplex ligands are mediated by R loops in human cancer cells.
647 *Proceedings of the National Academy of Sciences*, 116(3), 816–825.
648 <https://doi.org/10.1073/pnas.1810409116>
- 649 Mikhailova, A. A., Shamanskiy, V., Ushakova, K., Mikhailova, A. G., Oreshkov, S., Knorre, D., Tretiakov, E.
650 O., Zazhytska, M., Lukowski, S. W., Liou, C.-W., Lin, T.-K., Kunz, W. S., Reymond, A., Mazunin, I., Bazykin, G.
651 A., Gunbin, K., Fellay, J., Tanaka, M., Khrapko, K., & Popadin, K. (2020). Risk of mitochondrial deletions is
652 affected by the global secondary structure of the mitochondrial genome. *BioRxiv*, 603282.
653 <https://doi.org/10.1101/603282>
- 654 Miller, R. A. (2009). Cell Stress and Aging: New Emphasis on Multiplex Resistance Mechanisms. *The*
655 *Journals of Gerontology: Series A*, 64A(2), 179–182. <https://doi.org/10.1093/gerona/gln072>
- 656 Nissanka, N., Minczuk, M., & Moraes, C. T. (2019). Mechanisms of Mitochondrial DNA Deletion
657 Formation. *Trends in Genetics*, 35(3), 235–244. <https://doi.org/10.1016/j.tig.2019.01.001>

- 658 Oliveira, P. H., Silva, C. L. da, & Cabral, J. M. S. (2013). An Appraisal of Human Mitochondrial DNA
659 Instability: New Insights into the Role of Non-Canonical DNA Structures and Sequence Motifs. *PLOS ONE*,
660 8(3), e59907. <https://doi.org/10.1371/journal.pone.0059907>
- 661 Pacifici, M., Santini, L., Marco, M. D., Baisero, D., Francucci, L., Marasini, G. G., Visconti, P., & Rondinini, C.
662 (2013). Generation length for mammals. *Nature Conservation*, 5, 89–94.
663 <https://doi.org/10.3897/natureconservation.5.5734>
- 664 Pamplona, R., & Barja, G. (2007). Highly resistant macromolecular components and low rate of generation
665 of endogenous damage: Two key traits of longevity. *Ageing Research Reviews*, 6(3), 189–210.
666 <https://doi.org/10.1016/j.arr.2007.06.002>
- 667 Persson, Ö., Muthukumar, Y., Basu, S., Jenninger, L., Uhler, J. P., Berglund, A.-K., McFarland, R., Taylor, R.
668 W., Gustafsson, C. M., Larsson, E., & Falkenberg, M. (2019). Copy-choice recombination during
669 mitochondrial L-strand synthesis causes DNA deletions. *Nature Communications*, 10(1), 759.
670 <https://doi.org/10.1038/s41467-019-08673-5>
- 671 Puig Lombardi, E., & Londoño-Vallejo, A. (2020). A guide to computational methods for G-quadruplex
672 prediction. *Nucleic Acids Research*, 48(1), 1–15. <https://doi.org/10.1093/nar/gkz1097>
- 673 Richardson, A. G., & Schadt, E. E. (2014). The Role of Macromolecular Damage in Aging and Age-related
674 Disease. *The Journals of Gerontology: Series A*, 69(Suppl_1), S28–S32.
675 <https://doi.org/10.1093/gerona/glu056>
- 676 Shamanskiy, V. N., Timonina, V. N., Popadin, K. Yu., & Gunbin, K. V. (2019). ImtRDB: A database and
677 software for mitochondrial imperfect interspersed repeats annotation. *BMC Genomics*, 20(3), 295.
678 <https://doi.org/10.1186/s12864-019-5536-1>
- 679 Smith, R. (2019). Enhanced effective codon numbers to understand codon usage bias. *BioRxiv*, 644609.
680 <https://doi.org/10.1101/644609>
- 681 Solé, A., Delagoutte, E., Ciudad, C. J., Noé, V., & Alberti, P. (2017). Polypurine reverse-Hoogsteen (PPRH)
682 oligonucleotides can form triplexes with their target sequences even under conditions where they fold
683 into G-quadruplexes. *Scientific Reports*, 7(1), 39898. <https://doi.org/10.1038/srep39898>
- 684 Speakman, J. R. (2005). Correlations between physiology and lifespan – two widely ignored problems with
685 comparative studies. *Ageing Cell*, 4(4), 167–175. <https://doi.org/10.1111/j.1474-9726.2005.00162.x>
- 686 Tacutu, R., Thornton, D., Johnson, E., Budovsky, A., Barardo, D., Craig, T., Diana, E., Lehmann, G., Toren,
687 D., Wang, J., Fraifeld, V. E., & de Magalhães, J. P. (2018). Human Ageing Genomic Resources: New and
688 updated databases. *Nucleic Acids Research*, 46(D1), D1083–D1090. <https://doi.org/10.1093/nar/gkx1042>
- 689 Tadi, S. K., Sebastian, R., Dahal, S., Babu, R. K., Choudhary, B., & Raghavan, S. C. (2015). Microhomology-
690 mediated end joining is the principal mediator of double-strand break repair during mitochondrial DNA
691 lesions. *Molecular Biology of the Cell*, 27(2), 223–235. <https://doi.org/10.1091/mbc.e15-05-0260>
- 692 Toren, D., Barzilay, T., Tacutu, R., Lehmann, G., Muradian, K. K., & Fraifeld, V. E. (2016). MitoAge: A
693 database for comparative analysis of mitochondrial DNA, with a special focus on animal longevity. *Nucleic
694 Acids Research*, 44(Database issue), D1262–D1265. <https://doi.org/10.1093/nar/gkv1187>

- 695 Tremblay-Belzile, S., Lepage, É., Zampini, É., & Brisson, N. (2015). Short-range inversions: Rethinking
696 organelle genome stability. *BioEssays*, 37(10), 1086–1094. <https://doi.org/10.1002/bies.201500064>
- 697 Valencak, T. G., & Ruf, T. (2007). N-3 polyunsaturated fatty acids impair lifespan but have no role for
698 metabolism. *Aging Cell*, 6(1), 15–25. <https://doi.org/10.1111/j.1474-9726.2006.00257.x>
- 699 Wanrooij, S., & Falkenberg, M. (2010). The human mitochondrial replication fork in health and disease.
700 *Biochimica et Biophysica Acta (BBA) - Bioenergetics*, 1797(8), 1378–1388.
701 <https://doi.org/10.1016/j.bbabi.2010.04.015>
- 702 Yang, J.-N., Seluanov, A., & Gorbunova, V. (2013). Mitochondrial Inverted Repeats Strongly Correlate with
703 Lifespan: MtDNA Inversions and Aging. *PLOS ONE*, 8(9), e73318.
704 <https://doi.org/10.1371/journal.pone.0073318>